ELSEVIER

Journal of Non-Crystalline Solids 240 (1998) 1–21

JOURNAL OF NON-CRYSTALLINE SOLIDS

Microscopic origin of the glass forming tendency in chalcohalides and constraint theory

M. Mitkova [1], P. Boolchand *

Department of Electrical and Computer Engineering, and Computer Science, University of Cincinnati, Cincinnati, OH 45221-0030, USA

Received 16 February 1998; received in revised form 13 May 1998

Abstract

The glass forming tendency in two families of ternary glasses: the group IV-chalcohalides (such as Ge–S–I) and the Group V-chalcohalides (such as As–S–I) is analyzed. Predictions of the extended constraint theory, which explicitly includes the role of 1-fold coordinated (OFC) halogen atoms is cast in the form of universal compositional pathways along which the mean constraints per atom ($\bar{n}_c$) due to the nearest-neighbor (nn) covalent forces equals 3. When compared to the established glass forming compositions in more than 20 ternary glass systems, a correlation is observed with the predicted pathways. Notable exceptions also occur and reside away from the predicted compositions. The present analysis reveals that optimally constrained random networks occur along and in the vicinity of the predicted pathways, while near-optimally constrained molecular clusters occur at specific stoichiometries residing away from the predicted pathways. Molecular structure of Te chalcohalides is reviewed and the role of OFC-halogen atoms on the glass forming tendency is commented upon within the context of extended constraint theory.

Glossary

$\bar{r}$:	mean coordination number
$\bar{r}_c$:	critical mean coordination
nn:	nearest neighbor
$\bar{n}_c$:	mean constraints per atom
$\bar{n}_c = 3$:	optimally constrained network
$\bar{n}_c > 3$:	overconstrained network
$\bar{n}_c < 3$:	underconstrained network
T_ℓ:	liquidus temperature
T_g:	glass transition temperature
OFC:	one-fold coordinated atoms; in chalcohalides this represents a halogen atom σ bonded to one nearest-neighbor atom.
n_1/n:	fraction of OFC atoms in a network
GFT:	glass forming tendency
MDSC:	temperature modulated differential scanning calorimetry
Group IV chalcohalides:	$A_xB_{1-x-y}C_y$ ternary; A = tathogen, B = chalcogen; C = halogen; $\bar{n}_c = 3$ requires $y = (10x - 2)/3$ (line PQ)
Group V chalcohalides:	$D_xB_{1-x-y}C_y$ ternary; D = pnictide, B = chalcogen, C = halogen; $\bar{n}_c = 3$ requires $y = (5x - 2)3$ (line RS) if D is 3-fold, and $y = (7x - 2)/3$ (line TU) if D is quasi-4-fold coordinated

* Corresponding author. Tel.: +1-513 556 4758; fax: +1-513 556 7326; e-mail: pboolcha@ececs.uc.edu.

[1] Permanent address: Central Laboratory of Electrochemical Power Sources, Bulgarian Academy of Sciences, Sofia, Bulgaria.

0022-3093/98/$ – see front matter
PII: S0022-3093(98)00744-3

1. Introduction

1.1. Background

One of the remarkable discoveries of the past decade in glass science is the striking connection between physical behavior of a network glass with its connectivity, defined as the mean coordination number, $\bar{r}$. In chalcogenide glasses, formed by alloying a group V and/or a group IV element with a chalcogen, the correlation between physical properties and $\bar{r}$ was reviewed [1] recently. It was noted that the electronic, thermal, vibrational and structural properties change in a systematic manner with $\bar{r}$ until a threshold is observed near a critical $\bar{r}_c = 2.40$ where r_c is the magnitude of the critical mean coordination. Furthermore, the glass forming tendency as well appears to be correlated to $\bar{r}$ and is optimized when $r = \bar{r}_c = 2.40$. The microscopic origin of this behavior was traced to ideas on valence-force fields in these covalently bonded networks, which act as independent mechanical constraints [2,3]. And in particular, enumeration of these constraints with $\bar{r}$, reveals that the condition $\bar{r}_c = 2.40$ corresponds to a mechanical critical point

$$\bar{n}_c = 3 \tag{1}$$

when the number of mean-field constraints per atom ($\bar{n}_c$) equals three, the degrees of freedom per atom. Such a network is optimally constrained.

These elegant ideas on mean-field constraints were recently extended [4] to the case of networks containing terminal atoms, such as one-fold coordinated atoms (OFC-atoms) or dangling bonds. OFC-atoms have to be treated differently from atoms possessing a coordination number of 2 or higher because OFC-atoms do not contribute bond-bending constraints. For such networks, calculations [4] reveal that the condition $\bar{n}_c = 3$ is realized when

$$\bar{r}_c = 2.40 - 0.4(n_1/n), \tag{2}$$

where (n_1/n) represents the fraction of OFC-atoms in the network.

Chalcohalide glasses consist largely of alloys of group IV and group V chalcogenides with halogens (X = F, Cl, Br, I), although metal additives such as Ag, Ga, Hg, have also been used [5–8] in recent years. As anions, halogens in covalent systems are monovalent, and possess coordination number of one. Chalcohalide glasses appear to be ideal test systems for the new ideas on extended constraint theory since an extensive database exists on the glass forming regions [5–8] in a variety of these systems. In [4], one of us compared the prediction of constraint counting procedures (using Eq. (2)) with the known glass-forming tendency (GFT) in the Ge–S–I ternary [9]. We observed a correlation between the observed glass forming region and the parameter-free prediction of constraint theory.

1.2. Scope of present review

We have now reviewed glass forming regions in about 20 chalcohalide glass systems spanning two families, viz. one based on the group IV-chalcohalides (such as Ge–chalcogen–halogen) and the other based on the group V-chalcohalides (such as As–chalcogen–halogen). In this work we compare these experimental results with predictions of constraint theory taking the contribution of constraints due to OFC-halogen atoms explicitly [4,10]. We show that the correlation noted earlier for the Ge–S–I ternary is no accident, but forms part of a general trend observed in many other chalcohalides. Notable exceptions occur as well. The implications of this correlation or the lack thereof, has interesting consequences on the microcopic origin of glass formation. Here we should be careful not to jump to the conclusion that glass compositions residing away from the predicted compositions represent failures of constraint theory. On the contrary, many of the glass forming compositions residing away from the predicted compositional pathways can be traced to presence of particular molecular fragments that are not far from being optimally constrained [10]. We shall encounter such examples in the chalcohalides. The unusual nature of constraints imposed by OFC-halogen atoms when networks are either overcoordinated or undercoordinated was discussed in Ref. [10]. Constraint theory cannot predict the morphological structure of a network glass, i.e., whether a glass network possesses a homogeneous

microphase morphology, such as a random network or an intrinsically heterogeneous one consisting of multiple molecular phases, but it does exclude overcoordinated ($\bar{r} > 3$) or undercoordinated ($\bar{r} < 1.5$) molecular structures as viable structures present in good glasses.

In terms of applications, chalcohalide glasses have attracted interest [11] as low-loss infrared optical fiber materials and laser-hosts for rare-earths. Since some chalcohalide glasses can transmit up to 20 μm; waveguides based on select materials are attractive for delivering 10.6 μm radiation from a CO_2 laser for thermal imaging, medical and industrial cutting operations. Synthesis, chemical stability, structural characterization, optical transmission, and even some device applications of the chalcohalides have been the subject of numerous publications [12–16] in the Russian and East European literature, in addition to several recent review articles [5–8] in the Western literature. We have used this extensive database to analyze the molecular origin of glass formation in the chalcohalides. Comparison of the predictions of the extended constraint theory with the glass forming regions in the chalcohalide glasses has resulted in several new insights. It is in this respect the scope of the present review differs from the earlier reviews on the subject.

1.3. Definitions

We would like to define several terms (in italics) within the context of glass science and constraint theory at this stage. At the outset, we would like to state that the processing method, and in particular, the kinetic factors employed by various groups, in identifying the glass forming compositions in the examined ternaries, were kept the same. We have perused through the original citations, and have found that in each case glasses were synthesized by air-quenching macroscopic quantities (few grams or more) from above T_ℓ (liquidus temperature) of liquids melts, in a process that usually yields quench rates of about 10 K/s. Consequently, composition trends in glass forming tendency in various chalcohalides cannot be traced to kinetic factors but, as we suspect, largely originate due to changes in network connectivity as measured by $\bar{r}$.

Melts that can be supercooled at these low quench rates to yield glasses are usually reckoned in the glass science literature as *good glass formers*. Furthermore, in each case, since glasses were synthesized by melt-quenching macroscopic quantities (10 g or more) of liquid melts, such glasses will henceforth be denoted as *bulk glasses*. Such glasses are in contrast to glasses synthesized by splat cooling small droplets, or vapor deposited thin-films synthesized by evaporation or sputtering.

Within the context of chalcohalide glasses, the term OFC-atom refers to a halogen atom that enters into a σ-bond with a nearest-neighbor (nn) atom. Halogen atom bonding with more distant neighbors, will involve π-bonding and van der Waals interaction. The constraints associated with the second and more distant neighbors is considered to be broken, largely because the underlying bonding interactions are weaker than kT_g, where T_g is the glass transition.

Within constraint theory, a network is considered to be *optimally coordinated* if the mean coordination $\bar{r} = 2.40$. On the other hand, a network is considered over (under)-coordinated if $\bar{r} > (<) 2.40$. Bypassing crystallization to form a glass is thought to become difficult when networks are *highly overcoordinated*, i.e. $\bar{r} > 3.0$ or *highly undercoordinated*, i.e. $\bar{r} < 1.50$.

1.4. Outline of review

The outline of the paper is as follows. In Section 2 we identify the predictions of constraints theory for the two families of chalcohalides presently considered. In Sections 3 and 4, we compare these predictions with the published glass forming regions in the group IV and group V chalcohalides, respectively. About 20 ternary chalcohalide glasses are reviewed from a survey of the literature. TeX glasses, where X = halogen are of special interest within the context of OFC-atoms, and are treated separately in Section 5. We conclude with Section 6 identifying the principal results to emerge from this review.

2. Mean-field constraints in chalcohalide glasses

2.1. Ternary IV–VI–VII glassy alloys

Consider a ternary alloy system $A_xB_{1-x-y}C_y$ where the subscripts x, $1-x-y$, and y denote atomic percent concentrations of the group IV atom A, group VI atom B and group VII atom C. Atoms A, B and C possess a coordination number of 4, 2 and 1, respectively. For such a ternary, a compositional pathway can be established [4], along which the glass forming tendency is optimized, by requiring that the condition $\bar{n}_c = 3$, i.e., Eq. (1) can be satisfied. This equality is achieved by requiring the mean coordination, $\bar{r}$, be given by Eq. (2)

$$4x + 2(1-x-y) + y = 2.4 - 0.4y \quad \text{or}$$
$$y = (10x - 2)/3. \tag{3}$$

A plot of Eq. (3) is shown as the continuous line, PQ, in Fig. 1. The figure also displays the GFT in the Ge–S–I ternary [9]. Line PQ represents the parameter free universal prediction for the GFT of a IV–VI–VII ternary, based on mean-field constraint arguments. The linear relationship (3) connects point P, the $A_{0.20}B_{0.80}$ ($x = 0.20$, $y = 0$) binary composition with point Q, the $A_{0.38}C_{0.62}$ ($x = 0.38$, $y = 0.62$) binary composition. In discussing GFT, it will be instructive to supplement these strictly mechanical constraint counting arguments by chemical ones. Along the tie line PQ, we start with a network of $A(B_{1/2})_4$ tetrahedra with some B_n chains at the point P, and progressively form mixed tetrahedral units $A(B_{1/2})_{4-m}C_m$, $m = 1, 2$ and 3 and decoupled AC_4 units, as we approach the point, Q. The line, PQ, is thus the projection of the constraint counting procedure for a backbone of B_n chains and $A(B_{1/2})_4$ tetrahedra randomly terminated by halogen atoms. Constraint counting procedures merely rule out overcoordinated or undercoordinated molecular structures, but tell us little about the morphology of the optimally coordinated structures prevailing in the glasses. The latter is usually determined by free energy considerations of possible molecular structures formed at liquid densities. One of the challenges of glass science is to identify and then explain these molecular structures. A combination of structural probes, including diffraction methods, Raman scattering, NQR, Mössbauer spectroscopy and solid state NMR have been successful in this respect. In several cases, molecular fragments based on underlying crystalline phases form a basis for understanding the structure of glasses as will be illustrated later in discussing specific glass systems.

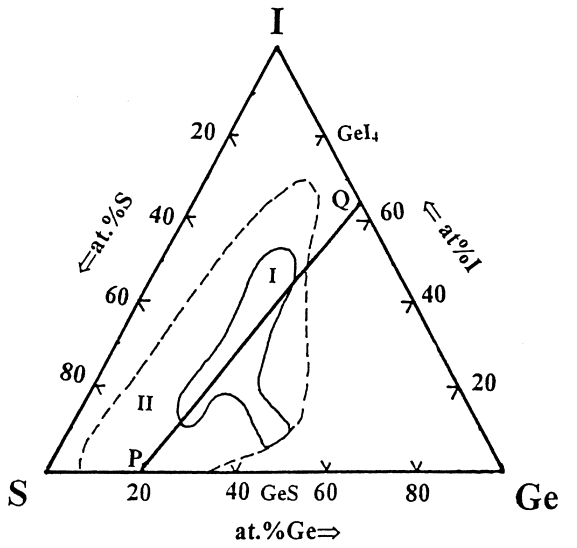

Fig. 1. Glass forming region in the Ge–S–I ternary taken from the work of Dembovsky et al. [9]. Glasses form in region II upon a water quench of melts. But of these only melt compositions in region I yield glasses when cooled very slowly at 2 K min^{-1}, showing that the glass forming tendency is optimized in region I. Line PQ is the prediction of the glass forming tendency based on Eq. (3) from extended constraint theory.

2.2. Ternary V–VI–VII glassy alloys

Consider a ternary alloy $D_xB_{1-x-y}C_y$ in which the group V atom D, group VI atom B and group VII atom C chemically bond with a coordination number of 3, 2 and 1, respectively. For such a ternary, the GFT is optimized when the mean coordination $\bar{r}$ of the network is given by Eq. (2), i.e.,

$$3x + 2(1-x-y) + y = 2.4 - 0.4y \quad \text{or}$$
$$y = (5x - 2)/3. \tag{4}$$

A plot of Eq. (4) is projected in Fig. 2 as the continuous line RS. Fig. 2 also displays the glass

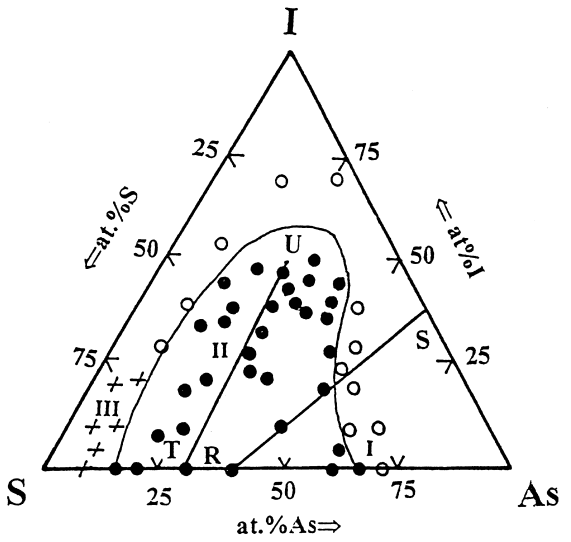

Fig. 2. Glass forming region in the As–S–I ternary taken from the work of Flaschen et al. [17]. Line RS is the prediction of the glass forming tendency based on Eq. (4) from extended constraint theory. The filled (open) circles represent glass (crystal) forming compositions. The (+) symbol represents glass compositions that are phase separated.

forming region in the As–S–I system [17–20]. The continuous straight line connects point R, corresponding to the binary composition, $D_{0.4}B_{0.6}$ ($x = 0.4, y = 0$), to the point S, corresponding to the binary composition $D_{0.62}C_{0.38}$ ($x = 0.62$, $y = 0.38$). At the point R, we visualize a network consisting predominantly of $D(B_{1/2})_3$ pyramids bridged across B sites. Progressive halogenation forms mixed $D(B_{1/2})_{3\text{-m}}C_m$, $m = 1$ and 2 pyramidal units, and eventually isolated and network decoupled DC_3 ones, as the point S is approached.

In several pnictide based chalcohalides, we can also encounter a 'phosphate type' of grouping in which the pnictide is quasi-tetrahedral, coordinated to three bridging and one non-bridging chalcogen. Thus, addition of phosphorus to a selenium glass, for example, leads to the formation of $PSe(Se_{1/2})_3$ units, in which three of the Se nn are bridging while one of the Se nn is non-bridging being coordinated to the phosphorus lone-pair of electrons.

For a ternary $D_xB_{1-x-y}C_y$ glass composed of chalcogen (B) chains, quasi-tetrahedral D units, and one-fold coordinated halogen atoms (C), we can predict glass compositions that are optimally constrained. This prediction is achieved by requiring that Eq. (2) be satisfied, i.e.,

$$4x + 2(1 - 2x - y) + x + y = 2.4 - 0.4(x + y) \quad \text{or}$$
$$y = (7x - 2)/3. \tag{5}$$

In deriving Eq. (5) we make use of the fact that there is one non-bridging chalcogen atom introduced in the network per pnictide cation and every halogen atom is one-fold coordinated. A plot of Eq. (5) appears in Fig. 2 as the continuous line, TU. Here it is interesting to observe that when $y = 0$, the critical pnictide concentration, $x = x_c = 2/7$, and it corresponds to the glass condition, $\bar{n}_c = 3$, in the binary chalcogenide D_xB_{1-x}. Along the line TU, we visualize a network of mixed quasi-tetrahedral $DB(B_{1/2})_{3-m}C_m$ units with B_n-chains to emerge as a function of halogen content of the glasses. A comparison of these ideas with the experimentally established glass forming regions in several pnictide based chalcohalides will be considered in the next section. This comparison will permit describing glasses in which a random network description is likely and in which a molecular cluster description more appropriate.

3. Glass forming tendency in group IV chalcohalides

Table 1 summarizes some of the known glass forming systems in the group IV chalcohalides. We could have included Sn- and Pb-based-chalcohalides in Table 1 as well, if some results on glass formation were available. The lack of results in this regard could either be due to difficulties of sample synthesis or possibly due to the lack of a systematic attempt to synthesize and describe all

Table 1
Glass forming systems in the indicated group IV chalcohalides investigated

Ternary	X = Cl	X = Br	X = I
Si–S–X	–	Poor [21]	Poor [22]
Si–Se–X	–	Fair [21]	V. good [21]
Si–Te–X	–	–	–
Ge–S–X	–	V. good [22]	V. good [9]
Ge–Se–X	–	Fair [22]	Good [21]
Ge–Te–X	–	–	Good [41]

the ternaries. Regardless, we hope that the limited results available on the subject will stimulate future activity in this fertile area.

3.1. Si–S–X (X = Cl, Br and I) ternary

Synthesis of Si–S–X ternary glasses appears to be difficult probably because of the vapor pressures of sulfur and the halogens. There may be alternate routes to synthesize these chalcohalide glasses other than a direct reaction of the elements. Binary Si–S glasses have been synthesized and have glass transition temperatures of 600 K or so. And there would appear to be no intrinsic difficulty to systematically react Si-halides and Si-chalcogenides in varying proportions to synthesize the Si-chalcohalides. At present we are not aware of any results. Iodides (X = I) of Si–S appear to have a higher liquidus and glass transition temperatures than the bromides (X = Br). We expect glass transition temperatures in these ternary systems to decrease with halogen content. It is possible that in the case of $SiSBr_2$ [21] and $SiSI_2$ [22] the glass transition temperatures T_g are <300 K. Synthesis of homogeneous glasses in these ternaries continues to be a challenge in which progress in the future is likely.

3.2. Si–Se–X (X = Cl, Br and I) ternary

We are aware of only one composition in the (X = Br) ternary, viz., $SiSeBr_2$, where an attempt [21] to synthesize a glass has been made. Unfortunately, the $SiSeBr_2$ composition is unstable in air, is a liquid at room temperature and solidifies slightly below room temperature, and thus probably T_g <300 K. Ternary Si–Se–Br melts with Br-content less than $SiSeBr_2$ should have a higher T_ℓ and T_g, and may be more amenable to forming glasses for study.

Glass formation in the X = I ternary is documented [21] in Fig. 3, and the observed trend in glass formation tracks the predictions of the extended constraint theory. The results also show that along the $(SiSeI)_{1-y}I_y$ join, glasses form up to $y = 0.5$ corresponding to a $SiSeI_{2.5}$ stoichiometry. The molecular structure of these ternary glasses has not been examined spectroscopically or by

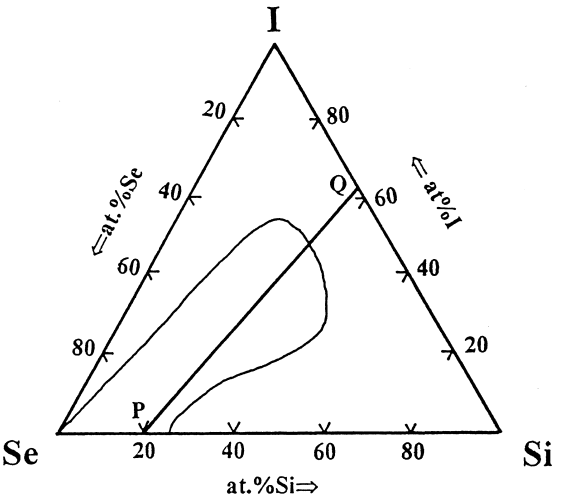

Fig. 3. Glass forming region in the Si–Se–I ternary taken from the work of Dembovsky and Popova [21], and compared to the prediction (line PQ) based on extended constraint theory.

diffraction methods. We suggest that the observed glass forming region shown in Fig. 3 indicates a molecular model [23,24]. At $Si_{0.2}$ $Se_{0.8}$ a network of corner-sharing and edge-sharing $Si(Se_{1/2})_4$ tetrahedra prevails, while upon iodine alloying, mixed tetrahedral units $Si(Se_{1/2})_{4-m}I_m (m = 1, 2$ and $3)$ emerge, and progessively depolymerize the network and eventually lead to phase separation of SiI_4 monomers from the network backbone. The latter is indicated by absence of bulk glass formation at high I content, particularly near the point Q, where constraint counting procedures predict glass formation, but none is actually documented.

3.3. Ge–S–X (X = Cl, Br, I)

Kirilenko et al. [22] attempted to synthesize a glass of $GeSBr_2$ composition by direct reaction of the elements at low temperatures but no clear conclusions emerged on glass formation. Koudelka and Pisarcik [25] and Heo and Mackenzie [26], on the other hand, successfully prepared (Fig. 4) ternary $(Ge_xS_{1-x})_{1-y}Br_y$ glasses over the compositions $(0 < x < 0.33, 0 < y < 0.70)$ using $GeBr_4$ and GeS_2 as starting materials. As expected, glass transition temperatures, examined at $x = 1/3$ and 0.25, decrease monotonically with Br con-

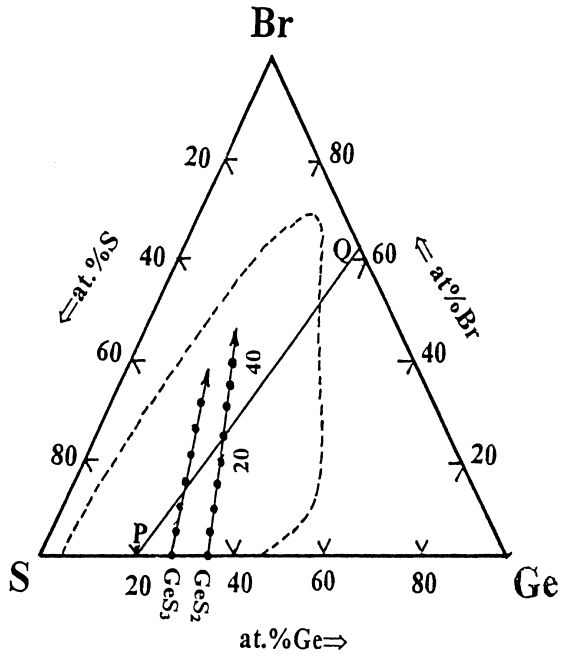

Fig. 4. Glass forming region in the Ge–S–Br ternary taken from the work of Kirilenko and Dembovsky [22], and compared to the prediction (line PQ) based on extended constraint theory. Physical behavior of ternary $Ge_xS_{1-x})_{1-y}Br_y$ glasses at $x = 1/4$ and $x = 1/3$, for y in the $0 < y < 0.40$ range represented by filled circles has been examined in Refs. [25,26].

centration, y. The $T_g(\bar{r})$ plot of Fig. 5(a) encompasses all their T_g results on a universal curve, and shows a correlation of T_g with network connectivity ($\bar{r}$). Such a correlation was noted earlier by Tatsumisago et al. [27] for chalcogenides, and these results on chalcohalides form a part of the same pattern. The $T_g(\bar{r})$ variation in chalcogenides and chalcohalides underscores the role of connectivity.

Heo and Mackenzie [26] have also reported on the density of the ternary glasses and observed it to increase with Br content. We have replotted their results in terms of molar volumes (Fig. 5(b)) and recognize that when the network connectivity, $\bar{r}$, increases to 2.4, molar volumes $V_M(\bar{r})$ decrease as the network is compacted. At $\bar{r} > 2.4$, two contrasting trends appear, one in which $V_M(\bar{r})$ continues to decrease with $\bar{r}$ and a second, in which $V_M(F)$ goes up with increasing $\bar{r}$, with $V_M(\bar{r})$ displaying a minimum [28] near $\bar{r} \simeq 2.4$. The former trend is observed in the present chalcohalide glasses, while the latter trend is documented in binary chalcogenide glasses [29]. This result is very curious. It is perhaps suggestive of the fact that in the binary chalcogenide system, molecular clustering occurs when at $\bar{r} \geqslant 2.40$, while in the ternary

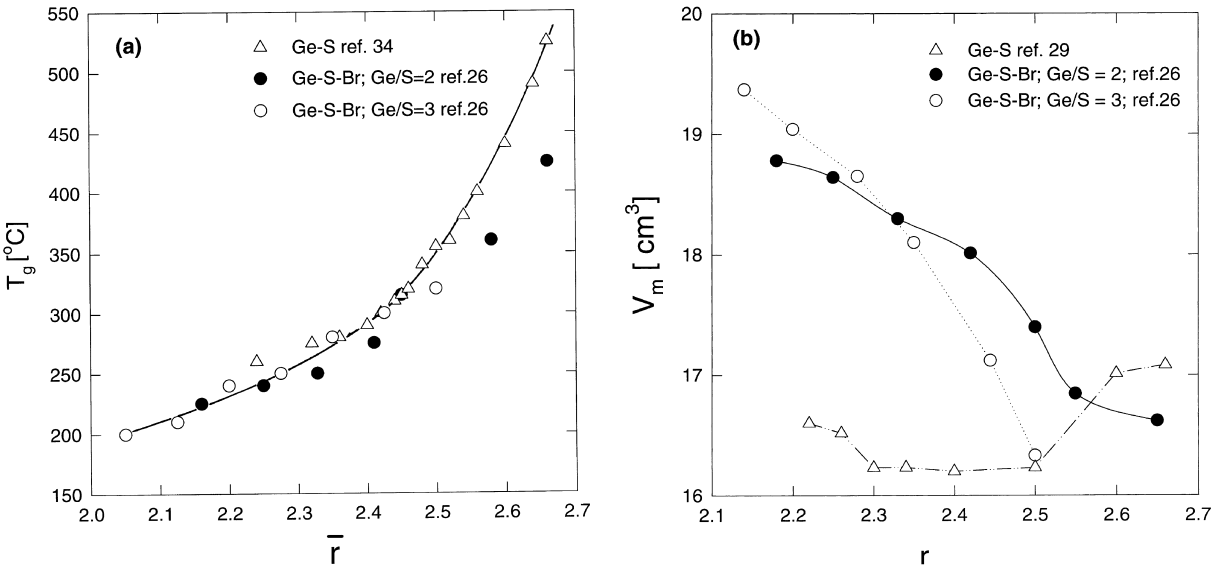

Fig. 5. (a) Glass transition temperature $T_g(\bar{r})$ variation as a function of mean coordination $\bar{r}$, in the $(Ge_xS_{1-x})_{1-y}Br_y$ chalcohalides (Ref. [26]) and chalcogenides (Ref. [34]) compared.(b) Molar volume $V_M(\bar{r})$ variation as a function of mean coordination $\bar{r}$ in the indicated chalcohalides (Ref. [26]) and chalcogenides (Ref. [29]) compared.

chalcohalide system, a random network morphology continues at $r > 2.40$. The role played by the glass compositions corresponding to $\bar{r} = 2.4$ is undoubtedly related to the floppy to rigid transition of the backbone [1]. These experimental results are fascinating and it would be of interest to pursue further, in a more quantitative fashion, the properties of these structure-related anomalies which are indicated by the stiffness transition in prototypical chalcohalides.

The glass forming tendency in the X = I ternary (Fig. 1), so elegantly described by the work of Dembovsky et al. [9], served as a benchmark for Boolchand and Thorpe [4] to compare the results of their theoretical predictions. Dembovsky et al. [9] were able to determine compositions at which the glass forming tendency was optimized by identifying liquid (melts) that form glasses even when cooled at a rate of 2 K/min. These particular liquid (melts) reside in region labelled I in Fig. 1. The striking overlap between region I and the predictions of constraint theory underscores the central role of optimally constrained random networks in promoting glass formation in the chalcohalides. Glass formation away from the line PQ and near the glass composition $(GeS)_{0.90}I_{0.10}$ may indicate nucleation of a specific floppy molecular fragment in this region, a point that merits further investigation.

Koudelka and Pisarcik [30], and Heo and Mackenzie [31] have examined the molecular structure of these glasses by Raman scattering and glass transition temperatures measured by scanning calorimetry. The Raman scattering data reveal pronounced changes especially in the region of 100–300 cm^{-1} with an increase in I content in $Ge_{0.3}S_{0.7-y}I_y$ glasses. Besides the dominant band at 340 cm^{-1}, identified with symmetric breathing of corner-sharing $Ge(S_{1/2})_4$ tetrahedral units, modes at 270, 230, 185 and 154 cm^{-1} are observed. The latter modes grow in scattering strength with increasing I content. These modes are ascribed respectively to the presence of mixed $Ge(Se_{1/2})_{4-m}I_m$ ($m = 1$, 2, 3 and 4) tetrahedral units, forming in the glasses. The loss of glass formation at largest I content, particularly near the point Q, is related to the formation of GeI_4 monomers that phase separate from the network backbone. These Raman scattering results on the Ge–S–I ternary provide convincing evidence for a random network of mixed tetrahedral units as a model description of these glasses along the PQ compositional pathway.

More recently, there have been efforts to quantitatively verify the predictions of the extended constraint theory. Viscosities (η) of ternary $(Ge_{0.3}S_{0.7})_{1-y}I_y$ glasses at specific iodine concentrations $y = 0$, 0.05, 0.10, 0.15 and 0.20 were reported by Seddon and Hemingway [32]. A Vogel–Fulcher plot of log η against T_g/T, according to the authors, reveals fragilities (slope d log η/dT) to be about the same at $x = 0$, 0.05 and 0.10, but to increase at $y = 0.15$ and at 0.20. For the titled glasses, one expects the stiffness threshold to occur when the mean coordination $\bar{r}$ fulfills Eq. (2), i.e.

$$\bar{r}_c = 2.4 - 0.4(n_1/N) \quad \text{or}$$
$$4(0.3 - 0.3y) + 2(0.7 - 0.7y) + x = 2.4 - 0.4y \quad \text{or}$$
$$y_c = 0.166 \qquad (6)$$

corresponding to 16.6 atomic percent of iodine in the titled ternary. It appears that the threshold in melt fragilities observed in these glasses [32] occurs between 10 and 15 at.% concentration range, and probably closer to 10 than to 15 at.% concentration. The difference between the observed and predicted stiffness threshold remains to be understood in those viscosity measurements. It may be that the lower fragility threshold is intrinsically related to the presence of S_8 monomers phase separating from the backbone upon I alloying.

Recently, Wells et al. [33] have examined ternary $Ge_{0.25}S_{0.75-y}I_y$ glasses in Raman scattering and temperature modulated differential scanning calorimetry experiments (MDSC). They probed the evolution of Raman mode frequencies and their strengths (Fig. 6), as well as the reversing and non-reversing heat flow at T_g, systematically as a function of iodine concentration, y, in the $0 < y < 0.30$ range. The vibrational modes observed as a function of iodine alloying (Fig. 6) bear a close analogy to the earlier work of Koudelka and Pisarcik [30], except Wells et al. [33] were able to observe the low frequency F_2 modes of the mixed tetrahedra as well because of the larger stray light rejection of their Raman spectrometers. The choice of these two experimental methods as a

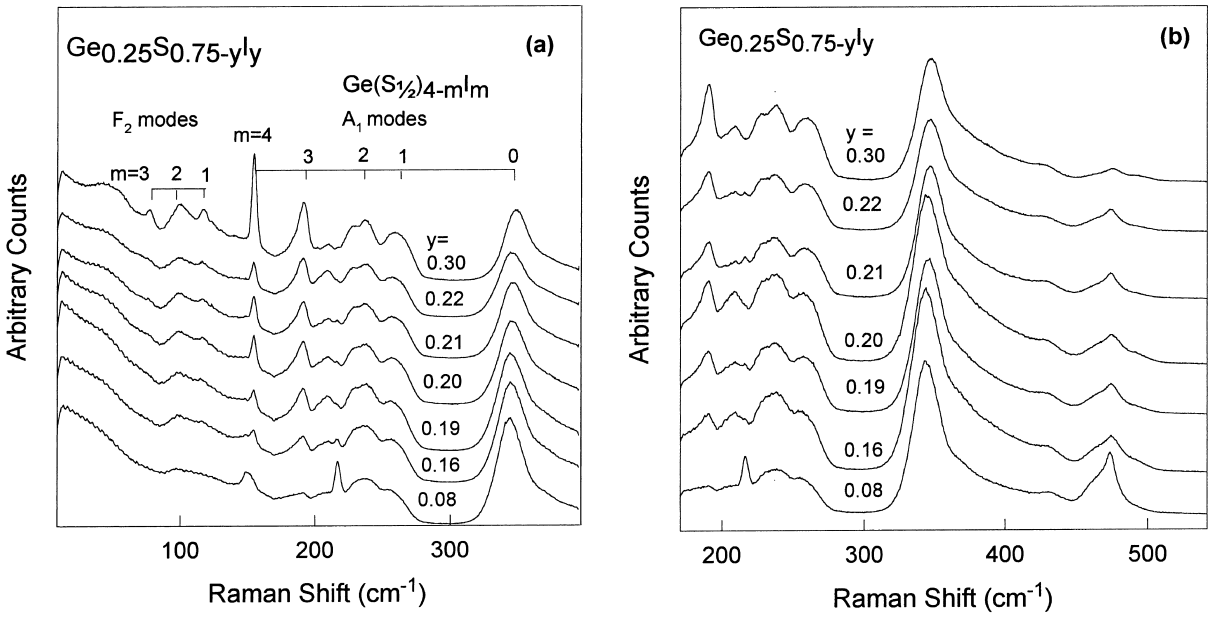

Fig. 6. Raman scattering results on indicated chalcohalide glasses taken from the work of et al. [33] showing evolution of vibrational modes of mixed tetrahedra and GeI_4 monomer (narrow mode at 154 cm^{-1}) with Iodine concentration. See text for details.

probe of the rigidity percolation threshold in binary chalcogenide glasses was highlighted by Feng et al. [34]. They observed an increase in frequency of the Raman A_1 symmetric stretch mode of $Ge(S_{1/2})_4$ and $Ge(Se_{1/2})_4$ tetrahedral units at $x = 0.23(1)$ in both Ge_xSe_{1-x} and Ge_xS_{1-x} glasses corresponding to the stiffness transition. Wells et al. have found that the Raman A_1 mode frequency of the symmetric stretch of $Ge(S_{1/2})_4$ tetrahedra in their ternary glasses also displays a threshold near $y = 0.20$, which correlates well with a minimum in the non-reversing heat-flow from the MDSC experiments. For the $Ge_{0.25}Se_{0.75-y}I_y$ ternary glasses ($x = 0.25$), the stiffness transition is predicated by Eq. (3) to occur at

$$y = (10x - 2)/3 \quad \text{or} \quad y = y_c = 0.166, \tag{7}$$

i.e., at 16.6 at.% of iodine. In the experiments of Wells et al. [33], some of the alloyed iodine does not enter the network backbone, as revealed by the formation of GeI_4 monomers displaying a narrow mode at 154 cm^{-1} in the Raman scattering experiments (Fig. 5(a)). When allowance is made for the phase separated iodine in the glasses, the observed and predicted stiffness thresholds are indeed quite close. The experiments of Wells et al. [33] thus provide quantitative support for ideas [4] on including the role of one-fold coordinated atoms explicitly in the counting of mechanical constraints in chalcohalide glasses.

3.4. Ge–Se–X (X = Cl, Br and I) ternary

We are aware of no results on the X = Cl ternary in this system. An attempt to synthesize a $GeSeBr_2$ glass by prolonged reaction of the elements at 400°C was reported [22]. However, the properties characteristics of the $GeSeBr_2$ glass sample were not reported.

Ternary Ge–Se–I glasses have been synthesized over a range of compositions by Dembovsky et al. [21] and from these results the glass forming region has been defined. These results have been refined more recently by Koudelka et al. [35] (Fig. 7). The refinements of Koudelka also conform with the known glass forming compositions in the Ge–Se binary noted by Feltz and Lippman [36]. The glass forming region obtained by Koudelka is consistent with the predictions of extended constraint theory. In contrast to the Ge–S–I ternary, there is no ev-

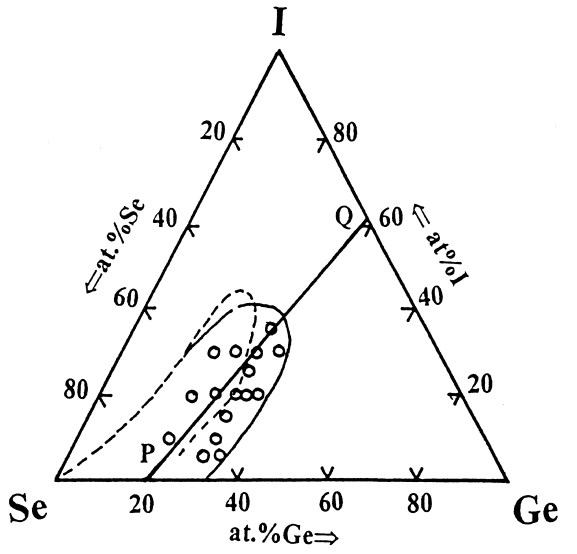

Fig. 7. Glass forming region in the Ge–Se–I ternary taken from the work of Dembovsky and Popova (broken line) [21] and Koudelka (continuous line) [35] compared to the prediction (line PQ) of extended constraint theory. The open circles represent the glass forming compositions according to Ref. [35]. See text for details.

idence of a glass forming region in Ge–Se–I ternary near the $(GeSe)_{0.9}I_{0.1}$ composition, perhaps indicating that the molecular phase present in the sulfide glasses is apparently not formed in the corresponding selenide glasses. A common feature of the glass forming regions in nearly all the Ge-chalcohalides ($Ge_xB_{1-x-y}C_y$) studied so far is that the $x = 1/4, y = 1/2$ composition (corresponding to the $GeBC_2$ stoichiometry) is close to the limit of glass formation. At this composition, we expect the backbone to consist predominantly of mixed tetrahedral $Ge(B_{1/2})_2C_2$ units. Although this particular building block is undercoordinated ($\bar{r} = 2$), a count of constraints per atom reveals that $\bar{n}_c = 2.5$, i.e. the network is marginally underconstrained. For a Se-chain glass, on the other hand, $\bar{r} = 2$ and $\bar{n}_c = 2$. The more constrained nature of the chalcohalide glass in relation to a Se-chain glass, stems from the constraints imposed by the OFC-halogen atoms [10].

The molecular structure of Ge–Se–I glasses has been examined in Raman scattering and in X-ray radial distribution functions [37]. The Raman scattering results on these Se-bearing glasses have close parallels to their S-bearing analogs, and in particular, provide evidence for mixed tetrahedral units emerging in the network upon Iodine alloying. The position of the first peak in the pair distribution function $g(r)$ moves from 0.238 to 0.242 nm upon iodine alloying. These results are consistent with replacement of Ge–Se bonds by Ge–I bonds in $Ge(Se_{1/2})_4$ tetrahedral units to form mixed tetrahedral units.

3.5. Ge–Te–X(X = Cl,Br,I) ternary

Bulk glass formation in the Ge_xTe_{1-x} binary occurs [38] in the composition range $0.14 < x < 0.23$. It is smaller than in corresponding Ge_xS_{1-x} and Ge_xSe_{1-x} glasses. The smaller glass forming range with Te anion in relation to S and Se anions, is an interesting result in its own right and we propose at least three factors that are responsible: (1) Liquid Te is 3-fold coordinated and metallic, while liquid S and Se are 2-fold coordinated and semiconducting. (2) c-$GeTe_2$ (in contrast to c-$GeSe_2$ or c-GeS_2) does not form a tetrahedrally coordinated network of $Ge(Te_{1/2})_4$ units, but disproportionates into more compact structures; c-Te and c-GeTe. Given these circumstances, it is remarkable indeed that bulk glass formation occurs in the Ge_xTe_{1-x} binary at all. (3) The glass forming tendency appears to be optimized near $x = 0.21$, and not the eutectic composition ($x = 0.15$) as revealed by a threshold in the ^{125}Te Lamb–Mössbauer factors [39]. We believe these results show that mechanical considerations along with chemical ones, drive supercooled liquids to become glassy. The mean coordination of liquid Te and liquid GeTe of 3 and 6, respectively, suggest mechanically overconstrained structures which are not conducive to glass formation. But a near equal mix of $Ge(Te_{1/2})_4$ tetrahedra with Te_n chains [40] in the vicinity of $x = 0.20$ provides an optimally constrained network (since $\bar{r} \sim 2.4$) and thus promotes glass formation. This result constitutes direct support for the constraint theory of glasses.

In the Ge–Te–I ternary, Feltz and Büttner [41] have documented bulk glass formation with up to 12 at.% of I as shown in Fig. 8. The experimentally established compositional trends for such glass

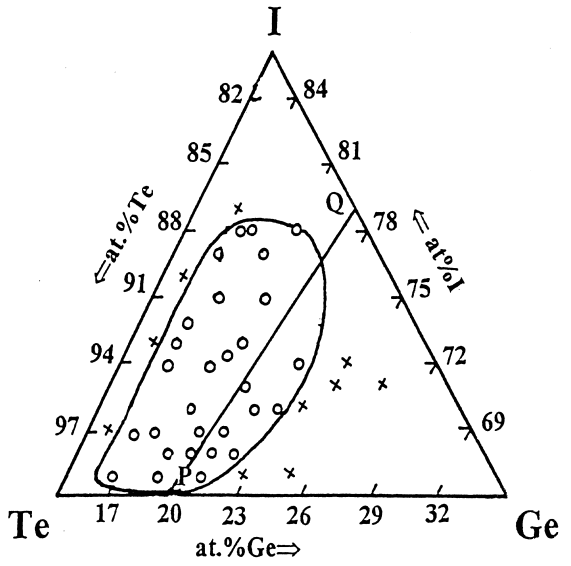

Fig. 8. Glass forming region in the Ge–Te–I ternary taken from the work of Feltz and Büttner [41] compared to the prediction (line PQ) of extended constraint theory. Open circles represent glass forming compositions, while the crosses represent partially crystalline compositions.

formation track the predicitions of extended constraint theory and suggest that I serves to randomly terminate the corner and edge-sharing tetrahedral network of $Ge(Te_{1/2})_4$ units prevailing at $x = 0.20$ [42].

4. Glass forming regions in group V-chalcohalides

Table 2 summarizes some of the known glass forming systems in the group V chalcohalides. The group V elements largely display 3-fold coordination with the chalcogens in a pyramidal configuration. Such a configuration is rather special when it comes to constraint counting, because it is optimally constrained with $\bar{n}_c = 3$. Not infrequently, examples of 4-fold coordination with the P-cation and 5-fold coordination with the Sb-cation are encountered in crystalline phases. Presence of such local bonding configurations has a profound impact on glass forming tendency as revealed from the experiments and, of course, as expected from constraint counting procedures.

4.1. P–Se–X (X = Cl, Br, I) ternary

Glass formation in the P_xSe_{1-x} binary occurs [43,44] over two compositional regions $0 < x < 0.52$ and $0.63 < x < 0.85$; these ranges are separated by a narrow window $0.52 < x < 0.63$, where crystallization results in a molecular solid composed of P_4Se_3 ($x = 0.57$) monomers even upon a fast quench of liquid (melts). Such monomers are overconstrained (see Table 3). Vibrational [45], thermal, solid state nuclear magnetic resonance [46] and diffraction methods [47] provide evidence for a variety of local building blocks as constituents of the binary glasses. Some of the local units include (a) quasi tetrahedral $PSe(Se_{1/2})_3$ units (in analogy to phosphate groupings in oxide glasses) having a non-bridging Se and three bridging Se, (b) pyramidal $P(Se_{1/2})_3$ units and (c) P_4Se_3 monomers and (d) P_4Se_5 monomers. the stoichiometries corresponding to these units, mean coordination number and mean constraints/atom are summarized in Table 3. The glass transition variation, $T_g(x)$, in the P_xSe_{1-x} binary in the $0 < x < 0.52$ range, has two maxima, one at $x = 0.29$ and the other at $x = 0.50$; the maximum at $x = 0.29$ is associated [48] with a network consisting of P_4Se_5 units with some Se chains, while the maximum at $x = 0.50$ is associated with P_4Se_3 units with some Se chains. These conclusions derive from diffraction and spectroscopic results [48]

Table 2
Glass forming systems in indicated group V chalcohalides investigated

Ternary	X = Cl	X = Br	X = I
P–S–X	–	–	–
P–Se–X	–	–	V. good [49,50]
As–S–X	Good [52]	Good [53]	V. good [54]
As–Se–X	–	Good [61]	V. good [62–64]
As–Te–X	–	Poor [67]	Good [63]

Table 3
Local units, stoichiometry, mean coordination and mean constraints/atom in the P–Se binary

Building block	P_xSe_{1-x} stoichiometry	$\bar{r}$	$\bar{n}_c$
Pseudotetrahedral 2[$PSe(Se_{1/2})_3$] dimer	0.28	2.28	3.0
Pyramidal $P(Se_{1/2})_3$	0.40	2.40	3.0
P_4Se_5 cage monomer	0.44	2.44	3.22
P_4Se_4 cage monomer (P_4Se_3+term.Se)	0.50	2.5	3.37
P_4Se_3 cage monomer	0.57	2.57	3.4
$P_{10}Se_6$ monomer	0.625	2.625	3.56

and appear to be in harmony with constraint counting considerations as illustrated in Table 3. Specifically, we note that T_gs increase with x displaying scaling with $\bar{n}_c$ in the $0 < x < 0.52$ composition range.

Iodine alloying in the binary P–Se glasses (Fig. 9) produces an extensive glass forming region [49] with an array of new molecular units [50] (Fig. 10) such as mixed pseudotetrahedral $PSe(Se_{1/2})_{3-m}I_m$ ($m = 1,2$ and 3), mixed pyramidal units $P(Se_{1/2})_{3-m}$ ($m = 1, 2, 3$) and finally $P_4Se_3I_2$ monomer based on P_4Se_3 monomer and PSe_2I molecular units based on P_2Se_5 parent unit.

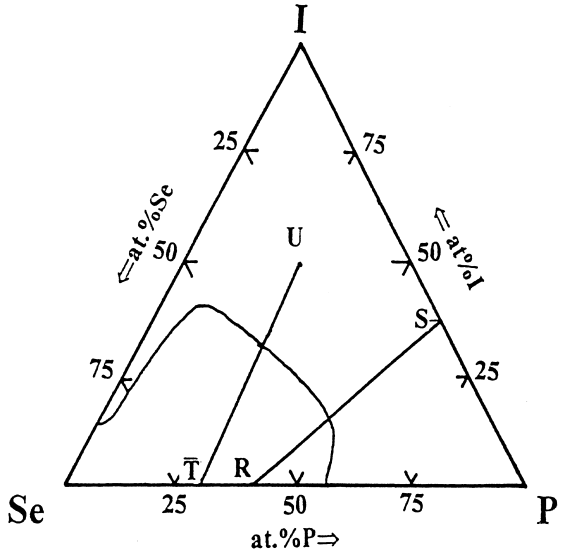

Fig. 9. Glass forming region in the P–Se–I ternary taken from the work of Dembovsky [49] and compared to the predictions (lines PQ and RS) of extended constraint theory. The large glass forming region is due to P cation acquiring 4-fold and 3-fold coordinated local structures as discussed in text.

Constraint counting algorithms serve to identify regimes of random network formation in the glass forming region. All molecular clusters encountered in these glasses are near optimally constrained in harmony with constraint counting algorithms. For example, both predicted pathways, TU and RS (Fig. 9), apply to the P–Se–I ternary since P cation can acquire both a modified 4-fold as well as 3-fold coordinated configurations with Se. One expects a random network of mixed pseudo tetrahedral $PSe(Se_{1/2})_{3-m}I_m$ local units to evolve along the pathway TU, and a random network of mixed pyramidal $P(Se_{1/2})_{3-m})I_m$ local units to evolve along the RS pathway. Glass formation near P:Se = 1 in Fig. 9 is most likely due to the characteristic molecular P_4SeI_2 fragment shown in Fig. 10(c). Glass formation at low-P content ($P:Se \leqslant 2:3$) and high iodine content, probably derives from the specific molecular fragments PSe_2I and/or $P_2Se_3I_2$ shown in Fig. 10(a). These considerations permit us to understand regions where random networks form and also regions where specific molecular clusters form in P–Se–I ternary chalcohalide glasses.

4.2. As–S–X (X = Cl, Br and I) ternary

Meyers and Felty [51] examined the glass forming tendency in binary As_xS_{1-x} glasses and showed one could form bulk glasses over the composition range $0 < x < 0.55$. In the binary glasses, $As(S_{1/2})_3$ pyramidal units along with S-chains and rings form the elements of structure, and one may expect halogens to terminate S chains and to progressively depolymerize the networks as mixed pyramidal $As(S_{1/2})_{3-m}I_m$ units; $m = 1, 2$ and eventually isolated AsI_3 pyramidal units emerge and phase separate from the network backbone.

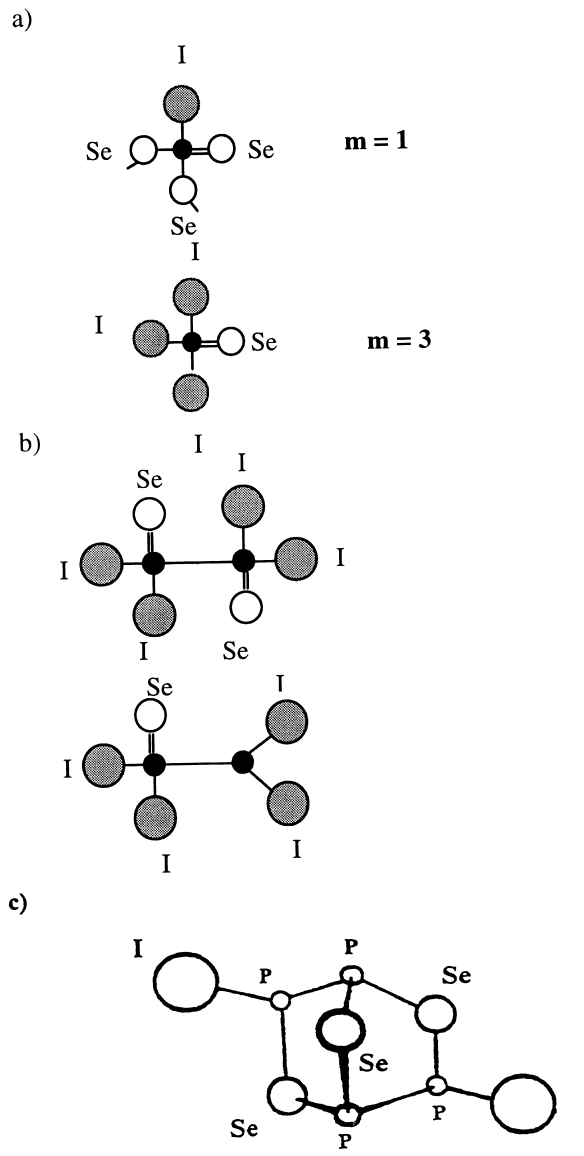

Fig. 10. Examples of mixed quasitetrahedral $PSe(Se_{1/2})_{3-m}I_m$ units (a) as building blocks of Se-rich P–Se–I glasses. In P-rich glasses of the ternary, possible local units containing P–P signatures are illustrated in (b) and (c).

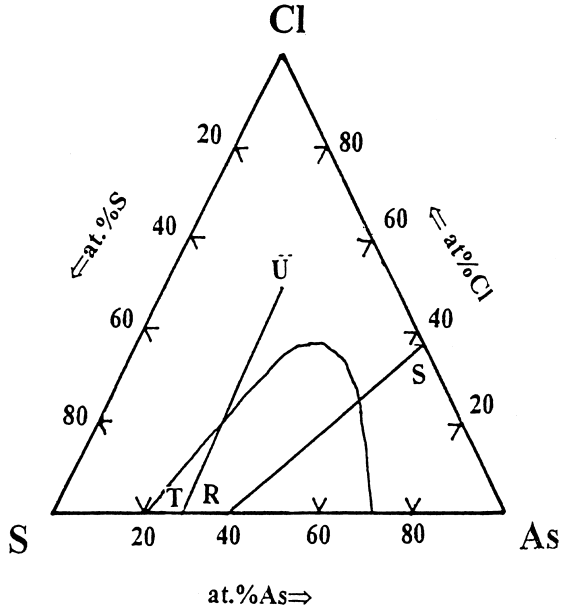

Fig. 11. Glass forming region in the As–S–Cl ternary taken from the work of Deeg et al. [52] compared to the predictions (line RS and line TU) of the extended constraint theory.

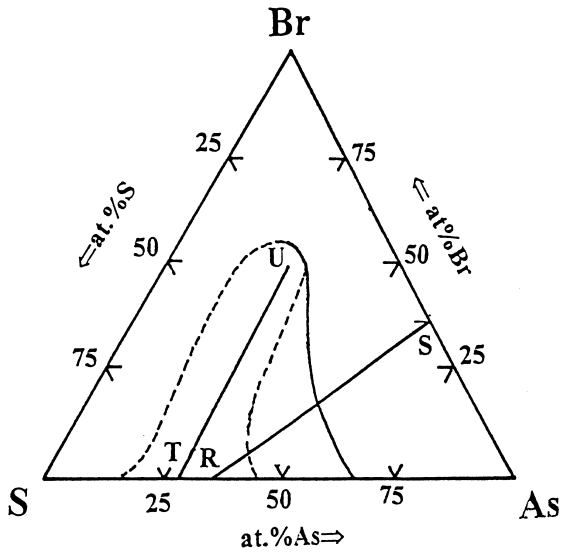

Fig. 12. Glass forming region (broken line) in the As–S–Br ternary taken from the work of Pearson et al. [53]. The continuous line is an estimate of the glass forming region by the present authors in the ternary based on the known (Figs. 11 and 13) glass forming compositions in the As–S binary. Lines RS and TU give the predictions of the glass forming tendency based on extended constraint theory.

The observed glass forming regions for the X = Cl, X = Br and X = I ternaries were studied, respectively, by Deeg et al. [52], Pearson et al. [53], and Flaschen et al. [17] and are displayed in Figs. 11 and 12 and 2. In general, we note that the correlation with extended constraint theory

predictions is good. The correlation underscores that along the predicted pathway RS, a backbone consisting of a random network of $As(S_{1/2})_{3-m}X_m$ building blocks is a reasonable molecular description of these glasses. At $y > 0.4$ bulk glass formation ceases along the line RS because of a preponderance of undercoordinated AsI_3 monomers [54] that are decoupled from the network.

In contrasting the role of the halogens on the glass forming regions, we note a pattern: glass formation occurs to the highest halogen content for the case X = I ternary ($y \simeq 0.60$) the lowest halogen content with X = Cl ternary ($y \simeq 0.40$) with the X = Br ternary falling in between these two extreme cases. The underlying process may derive from the larger polarizability of iodine in relation to chlorine, which makes feasible chemical bonds to form at the melting temperatures characteristic of these ternaries.

In comparing the glass forming region of the X = Br ternary (Fig. 12) taken from Ref. [53] with that of the X = Cl (Fig. 11) ternary taken from Ref. [52], we note that the range of glass formation at $y = 0$, i.e. in the As_xS_{1-x} binary between these two cases is not consistent with each other. Specifically, the absence of glass formation at $x > 0.45$ in the X = Br ternary (broken-line curve in Fig. 12), is clearly inconsistent with the known glass forming region in the X = Cl and X = I ternary. In our opinion, given these results, the continuous line in Fig. 12 is probably a more realistic glass forming range in the X = Br ternary. The molecular structure in the X = Br ternary has also been examined by Koudelka et al. [55,56] and their results are consistent with Br serving to interrupt the network by forming mixed $As(S_{1/2})_{3-m}Br_m$ pyramidal units ($m = 1$ and 2) in the glass forming compositions

Glass formation in the iodine bearing ternary is of special interest here. One finds from Fig. 2 that glass formation occurs predominantly along the pathway TU and to a lesser extend along RS. We suggest that these results show that mixed quasi tetrahedral $AsS(S_{1/2})_{3-m}I_m$ units are populated along TU. It is also apparent that a specific molecular fragment is present in the glasses at $x > 0.40$ that contains As–As bonds. A candidate molecular fragment is the $As_4S_3I_2$ monomer in analogy to $P_4S_3I_2$ [57] (Fig. 10), which has a mean coordination of 2.2 and a $\bar{n}_c = 2.78$.

The molecular structure of the iodine bearing ternary glasses has been examined in X-ray scattering and Raman scattering measurements by Hopkins et al. [18] and Koudelka et al. [20,58]. Their results are consistent with mixed $As(S_{1/2})_{3-m}I_m$ $(m = 1, 2)$ pyramidal units, and isolated AsI_3 units forming in the glasses with increasing iodine content. Furthermore, a bridging network of mixed $As(S_{1/2})_{3-m}I_m$ unit with $m = 1$, corresponding to AsSI stoichiometry ($\bar{r} = 2, \bar{n}_c = 2.33$) is a distinct possibility for the centroid composition ($As_{1/3}S_{1/3}I_{1/3}$) of the glass forming region.

In summary, the observed glass forming tendencies in the three ternaries X = Cl, Br and I compare well with predictions of the extended constraint theory. These results broadly reinforce that a random network of mixed quasi-tetrahedral units and pyramidal units form the principal structural elements in the ternary glasses. For the X = I ternary, molecular clusters based on $As_4S_3I_2$ stoichiometry could form the elements of medium range structure in the As-rich compositions $0.4 < x < 0.6$ at a finite lodine concentration $0 < y < 0.25$.

4.3. As–Se–X (X = Cl, Br and I) ternary

Binary As_xSe_{1-x} glasses can be synthesized in the $0 < x < 0.75$ composition range as demonstrated by several authors [51,59,60]. The molecular structure of these Se-bearing glasses in analogy to their S-analogues has been described in terms of Se-chains cross-linked at As sites to form pyramidal units. Near $x = 0.4$, the glass network is composed largely of pyramidal $As(Se_{1/2})_3$ units At $x > 0.4$, As–As signatures emerge probably in the form of As_4Se_4 units. In analogy to P_4Se_3, it is likely that As_4Se_3 monomers are populated in glasses near the $x = 0.60$ stoichiometry.

Given the structure of the binary glasses, we visualize halogen alloying to form a variety of mixed local units in which halogen atoms serve as OFC-terminal atoms. We are aware of no results on glass formation for the X = Cl ternary. Turyanitsa et al. [61] have examined the X = Br ternary,

and have shown that glasses containing up to $y = 0.40$ of the halogen can be synthesized (Fig. 13). To our knowledge, there are no structural investigations available on this ternary.

The X = I ternary has been studied by several authors [62–64] and there is unanimity on the glass forming region (Fig. 14) between the various authors. The observed glass forming compositions, conform nicely to the prediction of extended constraint theory.

A perusal of Fig. 14 also reveals that the glass forming range includes the mid-point composition $As_{1/3}Se_{1/3}I_{1/3}$. AsSeI crystallizes in a polymeric structure consisting of pyramidal $As(Se_{1/2})_2I$ units with a terminal I atom and a pair of bridging chalcogen sites (Fig. 15). Kanishcheva et al. [65] have isolated the structure of this ternary compound from single crystal investigations. This particular structure possesses a mean coordination $\bar{r} = 2$, but a count of mean constraints per atom reveals that $\bar{n}_c = 2.33$, i.e. a structure that is only marginally underconstrained. For these reasons the centroid composition displays affinity to form bulk glasses, not only in the present ternary but in a variety of other ternaries.

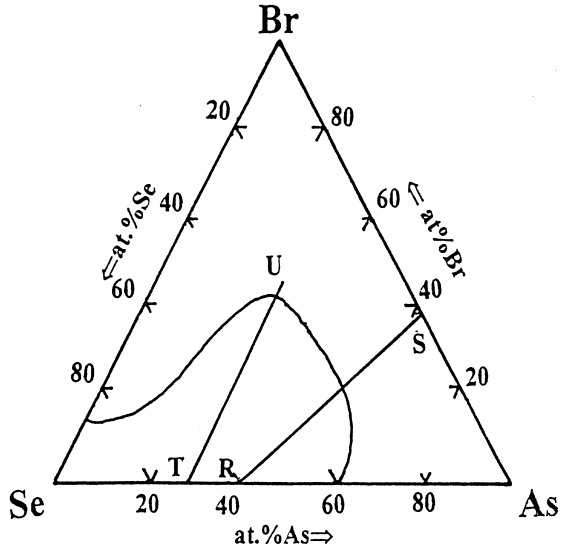

Fig. 13. Glass forming region in the As–Se–Br ternary taken from the work of Turynitsa et al. [61] compared to the predictions (lines RS and TU) of extended constraint theory.

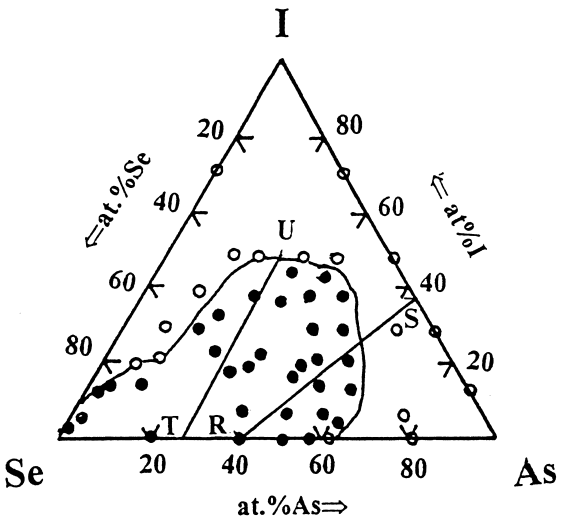

Fig. 14. Glass forming region in the As–Se–I ternary taken from the work of Munir et al. [63] compared to the predictions (lines RS and TU) of extended constraint theory. The filled circles represent glass forming compositions while open circles represent partially crystalline compositions.

The molecular structure of X = I ternary glasses has been examined by IR spectroscopy [66]. The results support the notion of mixed $As(Se_{1/2})_{3-m}I_m$ pyramids emerging as a function of iodine concentration, with the loss of glass formation as AsI_3 monomers appear in the network.

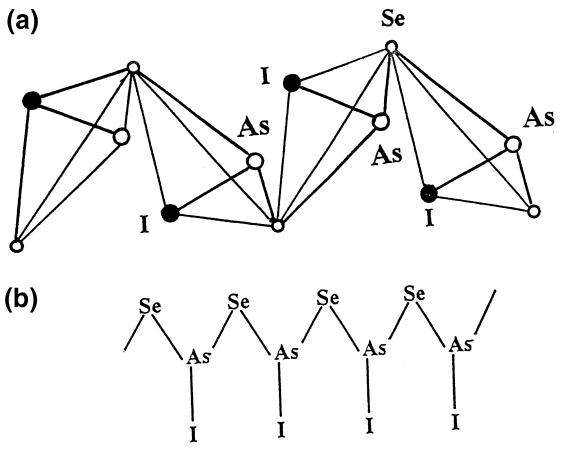

Fig. 15. Molecular structure of c-AsSeI (a) taken from Ref. [65] illustrating chains of pyramidal $As(Se_{1/2})_2I$ units bridged across Se sites. The bottom figure (b) illustrates the same structure schematically.

4.4. As–Te–X (X = Cl, Br,I)

In contrast to As–S–X and As–Se–X, the glass forming compositions in corresponding tellurides is much smaller, reflecting by and large the narrow glass forming range of the underlying As–Te binary. The suppressed glass forming tendency at $x = 0.40$ in the As_xTe_{1-x} binary is due to existence of the crystalline compound As_2Te_3, in which Te is 3-fold coordinated.

We are aware of no results with the X = Cl ternary. Turyanitsa et al. [67] have examined glass formation in the X = Br ternary and their results appear in Fig. 16. This incorporation of some Br in As_2Te_3 promotes glass formation, probably because molar volumes increase and the chalcogen Te becomes 2-fold coordinated as the chalcogens in As_2Se_3 and As_2S_3. The observed glass forming region is in reasonable accord with the prediction of the extended constrained theory.

Glass formation in the X = I ternary has been examined by Chernov et al. [68] and Fig. 17 summarizes their results. The glass forming compositions lie along the line RS and is in reasonable accord. The favorable glass compositions include $As(Te_{1/2})_{3-m}I_m$ units, and several other local units including As–As signatures, such as the ones shown in Fig. 18. In the ternary phase diagram the composition $As_4Te_5I_2$ displays a local maximum in T_g. This composition also resides at the heart of the glass forming range and it is likely that the local

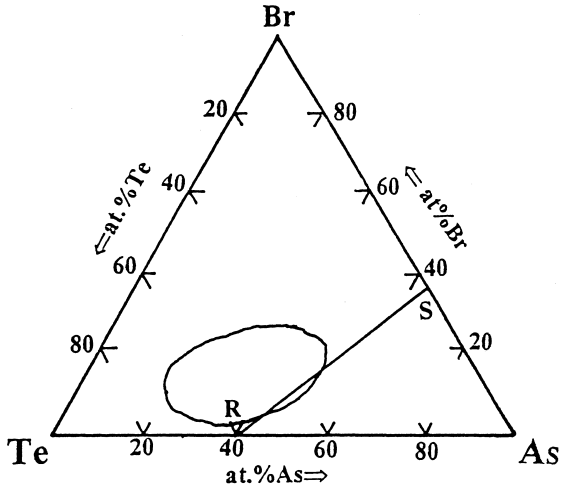

Fig. 16. Glass forming region in the As–Te–Br ternary taken from the work of Turyanitsa et al. [67] and compared to the prediction (line RS) of extended constraint theory.

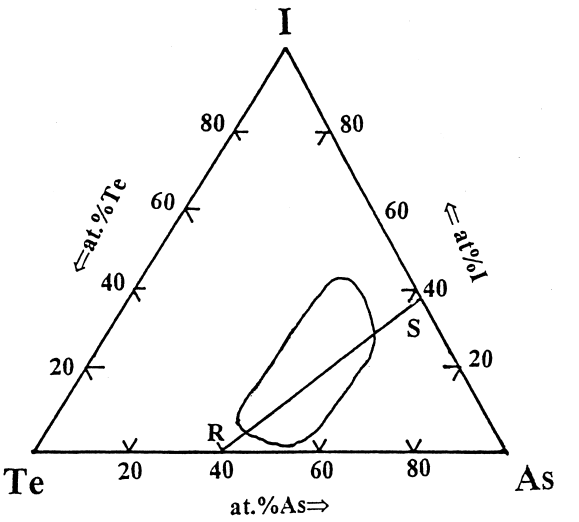

Fig. 17. Glass forming region in the As–Te–I ternary taken from the work of Chernov et al. [68] and compared to the prediction (line RS) of extended constraint theory.

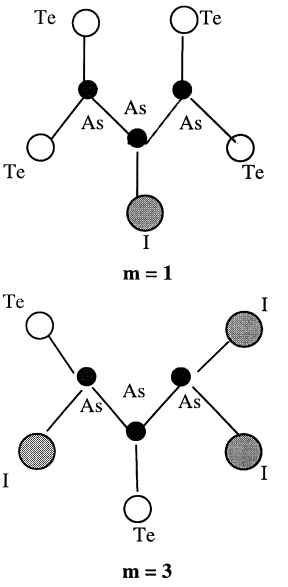

Fig. 18. Examples of mixed $As_3(Te_{1/2})_{5-m}I_m$ ($m = 1, 3$) local units as possible building blocks of As-rich glasses in the As–Te–I ternary taken from Ref. [68].

units of the molecular structure also form the elements of short-range of corresponding glasses.

5. Glass formation in Te-S(Se)-X,X = Cl, Br or I ternaries

The glass forming tendency in these ternaries has been the subject of recent interest [11], and compositions over which bulk glasses can be made by melt-quenching have been observed. These results are all the more interesting because liquids of Te in the elemental form, or as divalent or tetravalent chlorides, do not form glasses. But liquids of Te subhalides (Te_3Cl_2) which form unusual chain-like structures can be cooled to yield bulk glasses. Some of the glass forming compositions are illustrated for the Te–Se–X ternaries in Figs. 19–21. A perusal of these figures illustrates that glass formation occurs on the line joining the $Te_{0.6}X_{0.4}$ binary, X = Cl, Br and I, with elemental Se, highlighting the crucial role of the $Te_{0.6}X_{0.4}$ molecular structure in promoting glass formation.

The molecular strcuture of the stoichiometric $Te_{0.6}Cl_{0.4}$ glass has been compared to its crystalline counterpart by Wells et al. [69] using ^{129}I emission and ^{125}Te absorption Mössbauer spectroscopies. Crystalline $Te_{0.6}Cl_{0.4}$ consists of polymeric chains

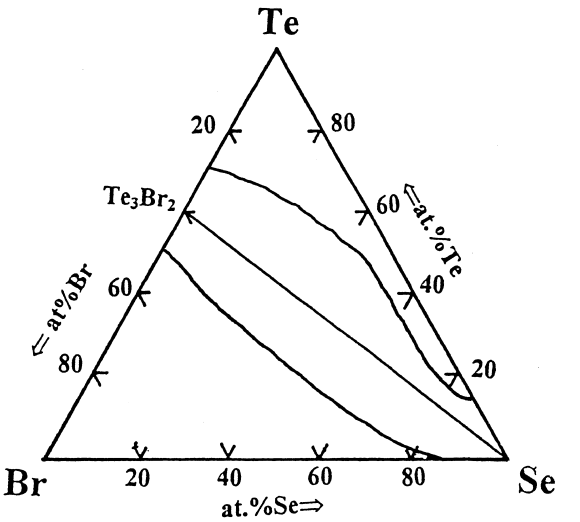

Fig. 20. Glass forming region in the Te–Se–Br ternary taken from the work of Lucas [11] showing glass formation to occur along the Te_3Br_2–Se join. Although crystalline possesses a high coordination number, g-Te_3Br_2 is known to occur as chain glass isomorphic to g-Te_3Cl_2.

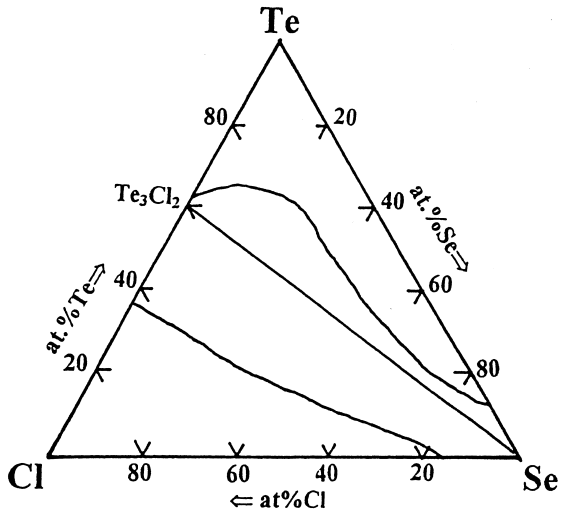

Fig. 19. Glass forming region in the Te–Se–Cl ternary taken from the work of Lucas [11] showing glass formation to occur along the Te_3Cl_2–Se join. Along this join glasses possess a chain structure ($\bar{r} = 2$) and the glass forming tendency is promoted by the floppiness of such structures.

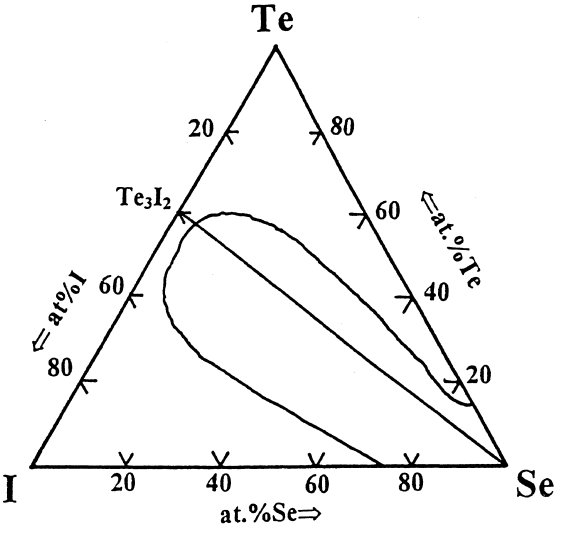

Fig. 21. Glass forming region in the Te–Se–I ternary taken from the work of Lucas [11] showing glass formation to occur along the Te_3I_2–Se join. The molecular structure of Te_3I_2 glass is not established, but it is speculated to be isomorphic to Te_3Cl_2.

of Te in which every third Te atom in a chain is 4-fold coordinated having a pair of Te nn along a chain and a pair of Cl ions as dangling ends (Fig. 22(a)). The Mössbauer experiments reveal that the $Te_{0.6}Cl_{0.4}$ stoichiometric glass consists of short-chain segments of 1.5 nm average length terminated by Cl ions as illustrated in Fig. 22(b).

We thus visualize the molecular structure of the $Te_{0.6-x}Se_xCl_{0.4}$ glasses as consisting of copolymeric chains in which Se replaces 2-fold coordinated Te sites along a chain. Bresser et al. [70] also showed that such Se substitution does not extend to the 4-fold coordinated parent Te sites in a chain, and in fact glass forming tendency declines once all 2-fold coordinated parent Te sites are replaced by Se. Apparently the polymeric $Se_{0.6}Cl_{0.4}$ chain structure is unstable against disproportionation into more compact structures consisting of the Se dihalide.

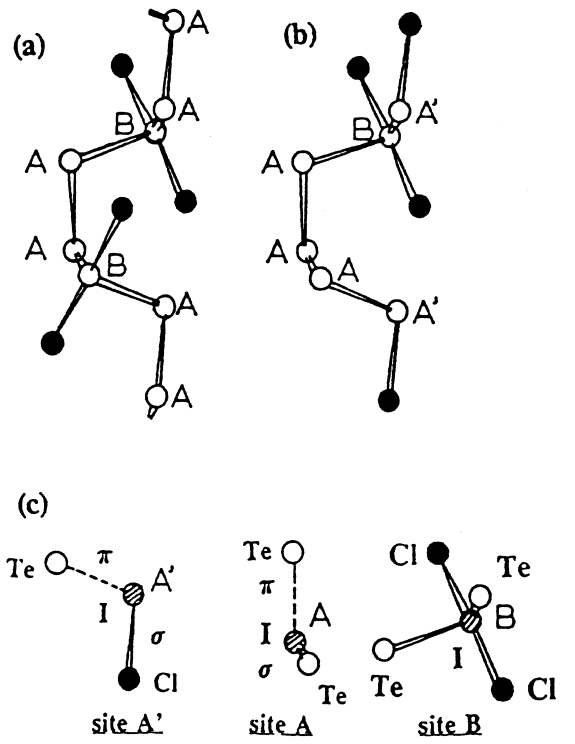

Fig. 22. Molecular structure (a) of c-Te_3Cl_2 and (b) g-Te_3Cl_2 deduced from ^{129}I Mössbauer spectroscopy measurements of Wells et al. [69] and (c) illustrates the trimodal site signatures observed in the spectroscopy.

The copolymeric chains are floppy because they are undercoordinated, possessing a mean coordiantion of $\bar{r} = 2$ regardless of composition. Mössbauer spectroscopy results show [69,70] that glasses in this ternary possess a chains structure, with the length of chains changing with the Se to Te ratio, but $\bar{r}$ always equals 2. These ideas on structure are compatible with the measured glass transition temperatures which are all between 70°C and 90°C for the $Te_{0.6}X_{0.4}$ (X = Cl, Br and I) binary and decline to about 30°C for elemental Se.

In contrast to bromides and chlorides, it is possible that glass formation in the Te–Se–I ternary is optimized along the TeI–Se join, instead of the Te_3I_2–Se join. TeI glass has been synthesized by melt-quenching [71] and has a $T_g = 33$°C. Less is known currently on the molecular structure of those glasses, although it may be of interest to remark that c-TeI is known to display two modifications with strikingly different molecular structures. And perhaps these crystal structures may have bearing on the molecular structure of corresponding glasses [72,73].

Constraint counting algorithms developed to include the role of OFC-atoms reveal that while these glasses are undercoordinated ($\bar{r} = 2$), they are not underconstrained to the same degree, however. In fact, a mean field count of nn bond-bending and bond-stretching constraints for a $Te_{0.6}Cl_{0.4}$ chain reveals that $\bar{n}_c = 2.4$. We would have obtained a smaller count ($\bar{n}_c = 2$) as in a Se chain glass, if one were to pluck all the one-fold coordinated Cl dangling ends and work with the skeletal chain network as some have advocated [74]. Use of the skeletal network to enumerate mechanical constraints/atom for underconstrained or overconstrained networks leads [10] to an underestimate in the former and an overestimate in the latter. The global decrease in the T_gs across the glass forming range (Figs. 19–21), starting from the left hand at $Te_{0.6}Cl_{0.4}$ ($T_g = 80$°C) and going to the right corner at Se ($T_g = 30$°c), appears to indicate that the former chains are more constrained ($\bar{n}_c = 2.4$) than the latter chains of Se ($\bar{n}_c = 2$). OFC-atoms stiffen a network if it is undercoordinated ($\bar{r} = 2$), these atoms soften a network if it is

overcoordinated ($\bar{r} = 4$) and play no part in either softening or stiffening a network if it is optimally coordinated ($\bar{r} = 2.4$) as discussed elsewhere [10]. The observed T_g variation in these ternaries supports the notion that even though all these glasses possess $\bar{r} = 2$, the degree to which they are underconstrained are not the same.

6. Conclusions

Phillips [2] introduced ideas on constraint theory of glasses. He suggested that the optimum glass forming tendency in the binary chalcogenide glass system, Ge_xSe_{1-x}, established near $x \simeq 0.20$ (or $\bar{r} = 2.4$) from minimum cooling rate experiments, provides evidence in support of the constraint theory. Recently, Boolchand and Thorpe [4] have extended constraint counting method to include networks with OFC-atoms. This development has made comparison of constraint theory based model predictions to the optimum glass forming compositions in chalcohalide glasses where the database fortunately is extensive in relation to the chalcogenides feasible. In this review, the prediction of the extended constraint theory has been compared to the observed glass forming regions in two families of ternary glasses; the group IV and the group V based chalcohalides. The documented glass forming regions in more than a score of ternary chalcohalide glass systems reveal an overlap with the predicted compositions based on enumeration of constraints. In many instances, glass formation is also found to occur at compositions far removed from the predicted compositions. We think that glass compositions residing near or close to the predicted compositions result from optimally constrained *random networks* with halogen atoms progressively terminating the network backbone. On the other hand, glass compositions residing away from the predicted compositions are also optimally constrained but consist of *molecular fragments* that are formed at specific stoichiometries controlled by the coordination chemistry of respective cations. A perusal of the available literature reveals a general pattern; although constraint theory cannot predict the morphology of the glass structure, it does impose bounds on possible structures. In none of the glass forming system investigated does one encounter overconstrained ($\bar{r} > 3$ or $\bar{n}_c > 4.5$) or underconstrained ($\bar{r} < 2$ or $\bar{n}_c < 2$) random networks or molecular clusters that form the backbone of a good glass former.

Acknowledgements

It is a pleasure to acknowledge correspondence with Dr Ladislav Koudelka, who provided new glass forming compositions in the Ge–Se–I ternary included in Fig. 6 and to Dr Jim Phillips for insights into chemical bonding of halogens and chalcogens. The present work is supported by the National Science Foundation grant DMR–92–07166 and DMR–97–01289, which has made possible for one of us to visit University of Cincinnati.

Note added in proof

We recently became aware of the work of G. Naunis and R. Kerner [75], who have developed a stochastic matrix description of T_g with network connectivity that provides a good physical basis to understand the results shown for example in Fig. 5(a).

References

[1] X. Feng, W.J. Bresser, M. Zhang, B. Goodman, P. Boolchand, J. Non-Cryst. Solids 222 (1997) 137.
[2] J.C. Phillips, J. Non-Cryst. Solids 34 (1979) 153.
[3] M.F. Thorpe, J. Non-Cryst. Solids 57 (1983) 355.
[4] P. Boolchand, M.F. Thorpe, Phys. Rev. B 50 (1994) 10366.
[5] J. Lucas, J.L. Adam, Glastech. Ber. 62 (1989) 422.
[6] J. Lucas, X.H. Zhang, J. Non-Cryst. Solids 125 (1990) 1.
[7] J.S. Sanghera, J. Heo, J.D. Mackenzie, J. Non-Cryst. Solids 103 (1988) 155.
[8] A.B. Seddon, J. Non-Cryst. Solids 213&214 (1997) 22.
[9] S.A. Dembovsky, V.V. Kirilenko, Y.A. Buslaev, Neorg. Mater. 7 (1971) 328.
[10] P. Boolchand, M. Zhang, B. Goodman, Phys. Rev. B 53 (1996) 11488.
[11] J. Lucas, X.H. Zhang, Mat. Res. Bull. 21 (1986) 871; also see J. Lucas, in: J. Zarzycki (Ed.), Glasses and Amorphous Materials, vol. 9, VCH, New York, 1991, p. 453.
[12] G.Z. Vinogradova, Glass Formation and Phase Equilibrium in Chalcogenide Systems, Nauka, Moscow, 1984.

[13] A. Feltz, Amorphous Inorganic Materials and Glasses, Weinhien, VCH, New York, 1993.
[14] A.S. Dembovsky and E.A. Chechetkina, Glass Formation, Nauka, Moscow 1990.
[15] M. Mitkova, T. Petkova, A. Janakiev, Mater. Chem. Phys. 30 (1991) 55.
[16] M. Mitkova, T. Petkova, Mater. Chem. Phys. 33 (1993) 233.
[17] S.S. Flaschen, A.D. Pearson, W.R. Northover, J. Appl. Phys. 31 (1960) 219.
[18] H. Maekawa, T. Maekawa, K. Kawamura, T. Yokokawa, J. Non-Cryst. Solids 127 (1991) 53.
[19] O.V. Khiminets, P.P. Puga, V.V. Khiminets, I.I. Rosola, G.D. Puga, Zh. Prikl. Spektr. 28 (1978) 700.
[20] L. Koudelka, M. Pisarcik, J. Non-Cryst. Solids 64 (1984) 87.
[21] S.A. Dembovsky, N.I. Popova, Izv. Acad. Nauk. SSSR-Neorg. Mat., 6 (1970) 138.
[22] V.V. Kirilenko, S.A. Dembovsky, Phys. Chem. Glass. 3 (1975) 225.
[23] S. Sugai, Phys. Rev. B 35 (1987) 1345.
[24] M. Tenhover, M.A. Hazzle, R.K. Grasselli, C.W. Thompson, Phys. Rev. B 28 (1983) 4608; J. Griffiths, M. Malyi, G.P. Espinosa, J.P. Rameika, Phys. Rev. B 30 (1984) 6978.
[25] L. Koudelka, M. Pisarcick, J. Non-Cryst. Solids 97&98 (1987) 1271.
[26] J. Heo, J.D. Mackenzie, J. Non-Cryst. Solids, 111 (1989) 29; 113 (1989) 1.
[27] M. Tatsumisago, B.L. Halfpap, J.L. Green, S.M. Lindsay, C.A. Angell, Phys. Rev. Lett. 64 (1990) 1549.
[28] S. Mahadevan, A. Giridhar, A.K. Singh, J. Non-Cryst. Solids 169 (1994) 133.
[29] Y. Kawamoto, S. Tsuchihashi, J. Am. Ceram Soc. 52 (1969) 626; 54 (1971) 131.
[30] L. Koudelka, M. Pisarcik, J. Non-Cryst. Solids 113 (1989) 239.
[31] J. Heo, J.D. Meckenzie, J. Non-Cryst. Solids 113 (1989) 246.
[32] A.B. Seddon, M.A. Hemingway, J. Non-Cryst. Solids 161 (1993) 323.
[33] J. Wells, W.J. Bresser, P. Boolchand, Bull. Am. Phys. Soc. 42 (1997) 249.
[34] Xingwei Feng, W.J. Bresser, P. Boolchand, Phys. Rev. Letts. 78 (1997) 4422.
[35] L. Koudelka, private communication to P. Boolchand.
[36] A. Feltz, F.-J. Lippmann, Z. Anorg. Allg. Chem. 398 (1973) 157.
[37] T. Usuki, O. Uemura, K. Fujimura, Y. Kameda, J. Non-Cryst. Solids 192&193 (1995) 69.
[38] J. Cornet, D. Rossier, J. Non-Cryst. Sol. 12 (1973) 61; 12 (1973) 85.
[39] R.N. Enzweiler, D. Salvanathan, P. Boolchand, unpublished.
[40] P. Boolchand, B.B. Triplett, S.S. Hanna, J.P. deNeufville, in: Irwin, J. Gruverman, C.W. Seidel, D.K. Dietely (Eds.), Mössbouer Effect Methodology, vol. 9, Plenum, New York, 1974, p. 53 .
[41] A. Feltz, H.J. Büttner, Z. Chem. 12 (1972) 392.
[42] D. Salvanathan, P. Boolchand, unpublished.
[43] R. Blachnik, A. Hoppe, J. Non-Cryst. Solids 34 (1979) 191.
[44] Y. Monteil, H. Vincent, Z. Anorg. Allg. Chem. 416 (1975) 181; 428 (1977) 259.
[45] R.T. Phillips, D. Wolverson, M.S. Burdis, Y. Fang, Phys. Rev. Lett. 63 (1989) 2574.
[46] H. Eckert, Angev. Chem. Int. Ed. Engl. Adv. Mater. 28 (1989) 1723.
[47] D.J. Verrall, S.R. Elliott, Phys. Rev. Lett. 61 (1988) 974.
[48] D.L. Price, M. Misawa, S. Susman, T.I. Morrison, G.K. Shenoy, M. Grimsditch, J. Non-Cryst. Solids 66 (1984) 443.
[49] A.S. Dembovsky, PhD thesis, Institute for General and Inorganic Chemistry of the Soviet Academy of Sciences, 1971, p. 65.
[50] M. Baudler, B. Volland, H.W. Valpertz, Chem. Ber. 106 (1973) 1049.
[51] M.B. Meyers, E.J. Felty, Mater. Res. Bull. 2 (1967) 535.
[52] E.V. Deeg, G.M. Habashy, R.O. Loufti, Spechsaal Keram. Glass, Email, Silikat 100 (1967) 757.
[53] A.D. Pearson, W.R. Northover, J.F. Devald, W.F. Peck, Advances in Glass Technology, vol. 2, Plenum, New York, 1962, p. 357.
[54] A.M. Bolotov, E.A. Bychkov, Yu.G. Vlasov, S.B. Rozenkov, F. Khalifa, Sov. J. Chem. Phys. 18 (1992) 470.
[55] L. Koudelka, J. Horak, M. Pisarcick, L. Sakal, J. Non-Cryst. Solids 31 (1979) 339.
[56] L. Koudelka. M. Pisarcik, Mater. Chem. Phys. 9 (1983) 571.
[57] G.J. Penney, G.M. Sheldrick, Acta Crystallogr. B 26 (1970) 2092.
[58] L. Koudelka, M. Pisarcik, Solid State Commun. 41 (1982) 115.
[59] T. Wagner, S.O. Kasap, Phil. Mag. B 74 (1996) 667.
[60] A. Kadoun, G. Chausoemy, J. Fernazero, J.M. Mackowski, J. Non-Cryst. Solids 57 (1983) 101.
[61] I.D. Turyanitsa, V.V. Khiminets, O.V. Khiminets, Fiz. Chim. Stekla 1 (1975) 170.
[62] V.N. Michailov, G.M. Orlova, L.I. Dojnikov, J. Prikl. Chimii. 44 (1971) 1152.
[63] Z.A. Munir, L.M. Fuke, E. Kay, J. Non-Cryst. Solids 12 (1973) 435.
[64] Z.U. Borisova in Glassy Semiconductors, 1981, Plenum, New York, p. 227.
[65] A.S. Kanishcheva, Yu.N. Mikhailov, A.P. Chernov, Sov. Phys. Dokl 25 (1980) 234.
[66] O.V. Khiminets, V.S. Gerassimenko, V.V. Khiminets, J. Prikl. Chimii. 5 (1978) 1522.
[67] I.D. Turyanitsa, V.V. Khiminets, O.V. Khiminets, I.D. Turyanitsa, K.I. Pinsenik, Fiz. Chim. Stekla 1 (1975) 170.
[68] A.P. Chernov, S.A. Dembovsky, N.P. Luzhnaja, Russ. J. Inorg. Chem. 20 (1975) 1208.

[69] J. Wells, W.J. Bresser, P. Boolchand, J. Lucas, J. Non-Cryst. Solids 195 (1996) 170.
[70] W.J. Bresser, J. Wells, M. Zhang, P. Boolchand, Z. Naturforsch a51 (1996) 373.
[71] J. Wells, W.J. Bresser, P. Boolchand, Bull. Am. Phys. Soc. 41 (1996) 291.
[72] W.R. Blackmore, S.C. Abrahams, J. Kainajs, Acta Crystallogr. 9 (1956) 295.
[73] R. Kniep, thesis, Universität Braunschweig, 1973; also see R. Kniep, D. Mootz, A. Rabeneau, Z. Anorg, Allg. Chem. 422 (1976) 17.
[74] M.F. Thorpe, J. Non-Cryst. Solids 182 (1995) 355.
[75] G.G. Naumis, R. Kerner, J. Non-Cryst. Solids 231 (1998) 111.